Supporting information

Efficient artificial light-harvesting systems based on aggregation-induced emission constructed in supramolecular gels

Xinxian Ma*[a], Bo Qiao[a #], Jinlong Yue[a], JingJing Yu[a], Yutao Geng[a], Yingshan Lai[a], Enke Feng[a], Xinning Han[a], Minghua Liu*[b]

[a.]College of Chemistry and Chemical Engineering, Ningxia Normal University, Guyuan 756000, People's Republic of China.E-mail: maxinxian@163.com;Tel: +86-954 2079637;

[b.]CAS Key Laboratory of Colloid, Interface and Chemical Thermodynamics, Institute of Chemistry, Chinese Academy of Sciences, Beijing, P. R. China. E-mail: liumh@iccas.ac.cn; Tel: +86-10-82615803

Materials

1. Instrumentation and methods

All reactions were taken place in the air except as otherwise noted. All measurements were carried out at room temperature. All chemicals were used without further purification, unless otherwise noted. 2-nonyl-benzimidazole-3-butyryl hydrazide was purchased from BJ Carbene Technology Co. Ltd. Dibenzothiophene-4-Carboxaldehyde was purchased from Shanghai Titan Scientific Co. Ltd.. Acridine red was purchased from SHANGHAI CANSPEC S&T CO. LTD.. Rhodamine B was purchased from China Pharmaceutical Corporation Beijing Purchasing and Supply Station.

NMR spectra were carried out on a Bruker 400MHz spectrometer with internal standard tetramethylsilane (TMS) and solvent signals as internal references at room temperature, and the chemical shifts (δ) were showed in ppm. The HRMS spectra were carried out on Aglient6550qtof & Thermo Fisher-QE. The morphologies of the

synthesized samples were characterized with a JSM-6701F SEM using an accelerating voltage of 5kV. The UV-Vis absorption spectra were measured on UV-1750 spectrophotometer. The fluorescence spectra were measured on RF-6000 instrument. The quantum yields were measured on a FLS980 fluorescence spectrometer. The fluorescence microscopywere performed with Olympus IX 71.

2. Synthesis and characterization of compound 1

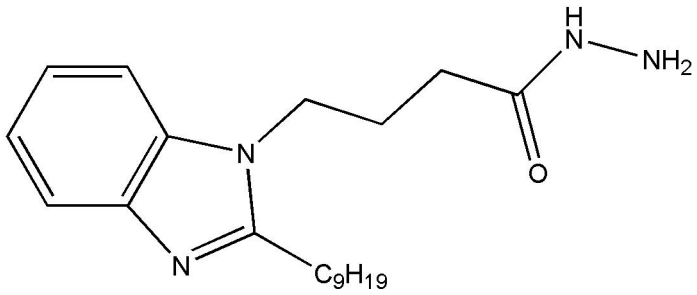

Scheme S1. Synthesis of compound 1

Compound 1 was synthesized according to literature reports. ^{1}H NMR (400 MHz, DMSO-d_6) δ (ppm) : 8.95 (s, 1H), 7.49 (ddd, J=8.1, 7.2, 1.3 Hz, 2H), 7.17-7.07 (m, 2H), 4.21 (s, 2H), 4.16-4.07 (m, 2H), 2.80 (t, J=7.6 Hz, 2H), 2.08 (t, J=7.2 Hz, 2H), 1.94-1.83 (m, 2H), 1.81-1.71 (m, 2H), 1.42-1.16 (m, 12H), 0.83 (t, J = 6.8 Hz, 3H). ^{13}C NMR (100.5 MHz, DMSO-d_6) δ (ppm) : 171.25, 155.28, 142.86, 135.43, 121.74, 121.49, 118.77, 110.38, 42.69, 31.73, 30.44, 29.39, 29.30, 29.27, 29.14, 27.49, 26.78, 25.76, 22.54, 14.39.

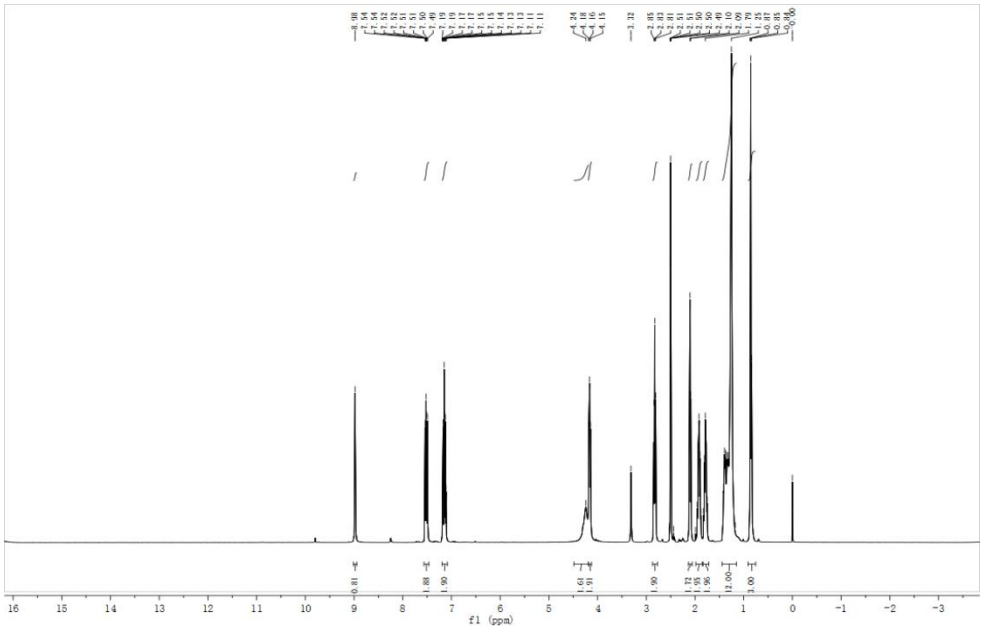

Fig. S1. ^{1}H NMR (400 MHz) spectrum of compound 1 in DMSO-d_6 at 25°C

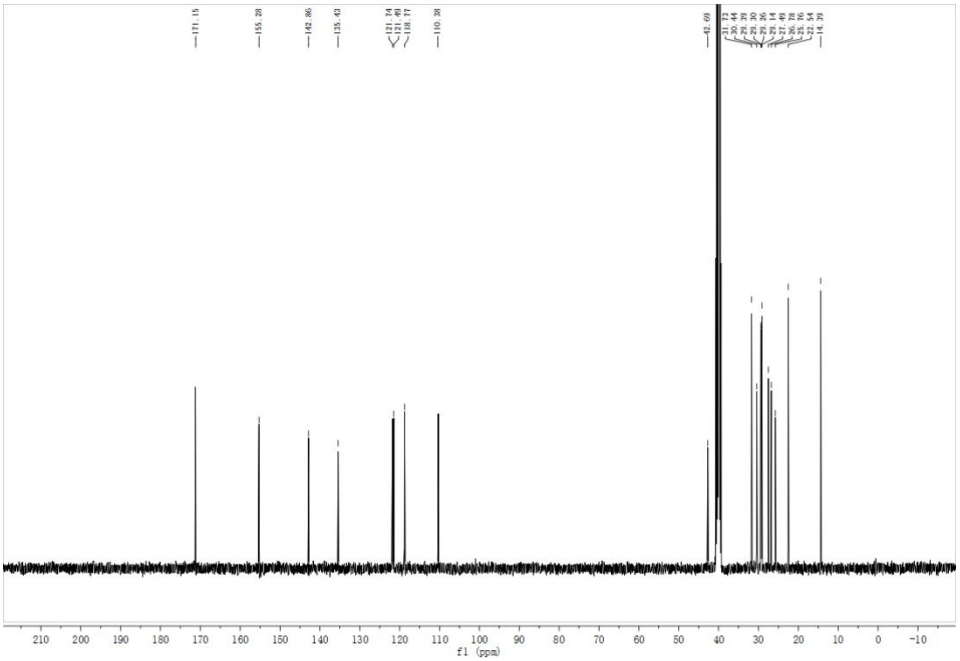

Fig. S2. ^{13}C NMR spectrum of compound 1 in DMSO-d_6 at 25°C

3. Synthesis and characterization of Gelator G2

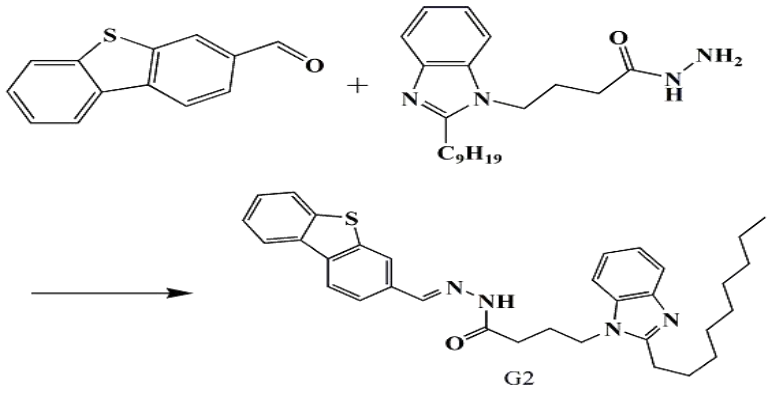

Scheme S2. Synthesis of Gelator G2

Synthesis of Gelator G2: 2- nonyl-benzimidazole-3-butyryl hydrazide (7.30 g, 0.02 mol) was mixed with Dibenzothiophene-4-Carboxaldehyde (4.50 g, 0.02 mol) in DMF solution and was refluxed for 8 h. After the reaction mixture was cooled to room temperature, the mixture was added to distilled water and lots of solid powder was precipitated by filtration. Then the precipitate was filtered and washed with ethyl alcohol, then dried under vacuum to gelator G2. Yield: 10.12 g (86%) .

^{1}H NMR (400 MHz, DMSO-d_6) δ (ppm): 11.59 (d, J=26.3 Hz, 1H), 8.57-8.29 (m, 3H), 8.12 (dd, J=61.7, 7.2 Hz, 1H), 7.75-7.47 (m, 6H), 7.21-7.05 (m, 2H), 4.42-4.21 (m, 2H), 2.99-2.80 (m, 4H), 2.21-2.04 (m, 2H), 1.83-1.67 (m, 2H), 1.15 (dd, J=51.6, 20.8 Hz, 12H), 0.75 (t, J=6.9 Hz, 3H).

^{13}C NMR (100.5 MHz, $CDCl_3$) δ (ppm): 175.34, 155.54, 143.80, 142.87, 141.22, 137.28, 135.44, 135.36, 134.82, 129.82, 128.44, 127.52, 125.09, 124.75, 123.43, 123.13, 122.38, 122.17, 121.89, 119.45, 109.79, 43.55, 32.18, 30.42, 29.96, 29.77, 29.76, 29.59, 28.25, 27.88, 25.02, 22.97, 14.43.

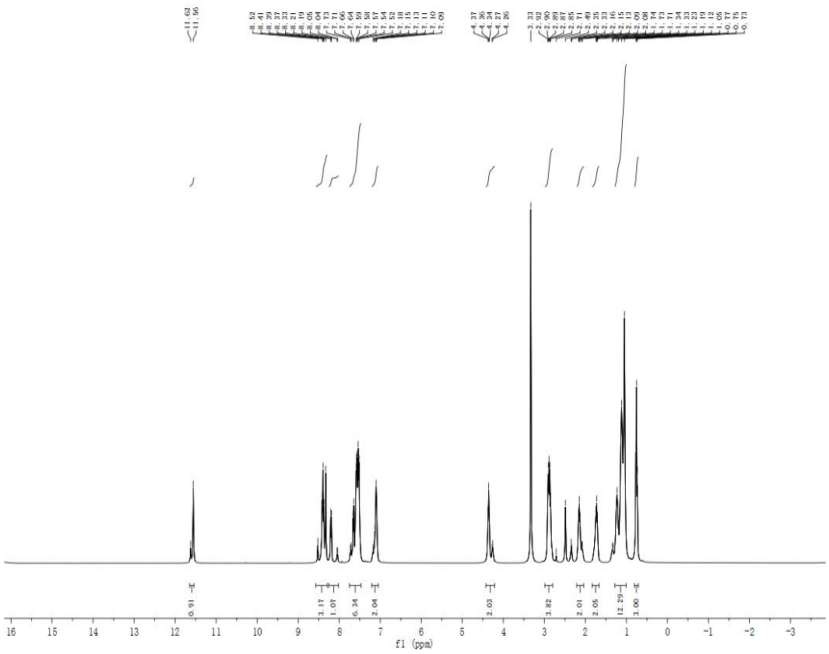

Fig. S3. ^{1}H NMR (400 MHz) spectrum of gelator G2 in DMSO-d_6 at 25°C

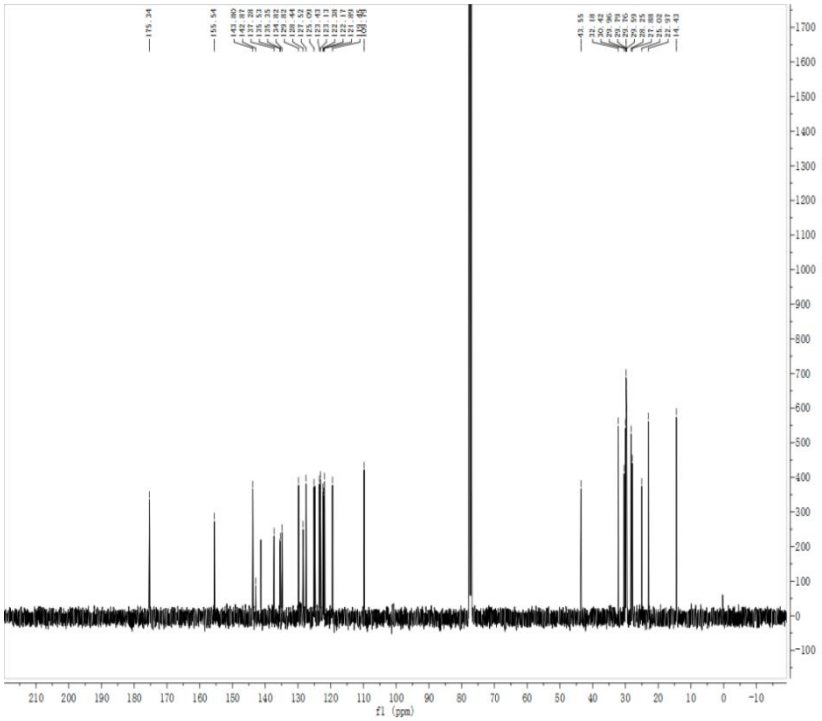

Fig. S4. ^{13}C NMR spectrum of gelator G2 in $CDCl_3$ at 25°C

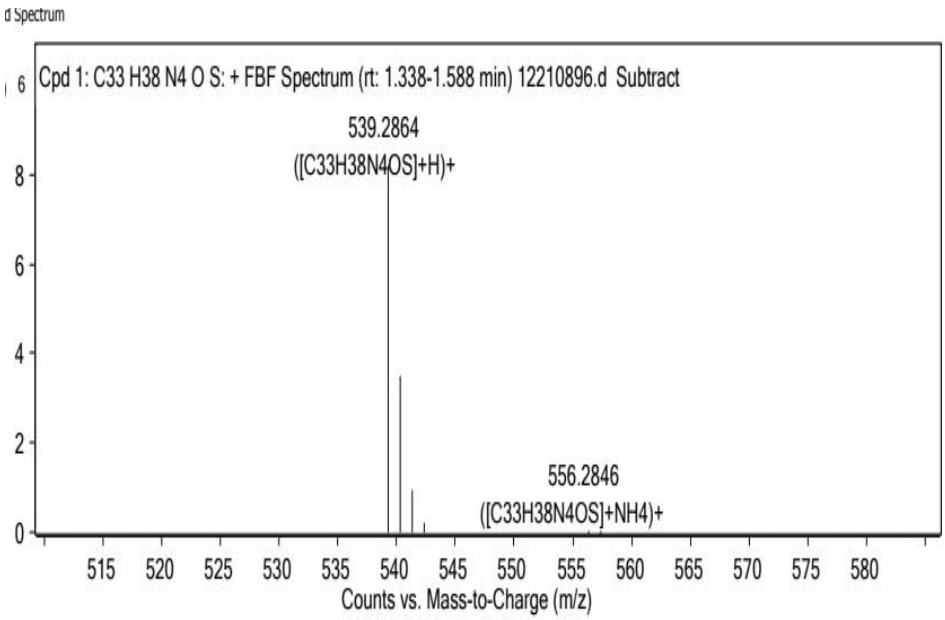

Fig. S5. HRMS spectra of gelator G2

4. Gelation property of gelator G2

Table S1. Gelation property of gelator G2

Entry	Solvent	State[a]	CGC[b]
1	n-Butyl alcohol	S	\
2	Propyl alcohol	G	0.3
3	Ethanediol	G	0.1
4	Ethyl acetate	P	\
5	Acetonitrile	P	\
6	Methanol	P	\
7	Clycerol	P	\
8	Isoamyl alcohol	S	\
9	Isopropanol	P	\
10	Dichloromethane	P	\
11	Ethanol	P	\
12	DMF	S	\
13	DMSO	S	\
14	Cyclohexane	P	\
15	Petroleum ether	P	\
16	Tetrahydrofuran	S	\
17	Chloroform	S	\
18	Acetone	P	\
19	Hexyl alcohol	G	0.2
20	n-butyl alcohol	G	0.3

[a]G, P, and S denote gelation, precipitation, fluid, part gelation and solution, respectively

[b]The critical gelation concentration(wt %, 10 mg/mL)

5. The thermally reversible of the G2@gel

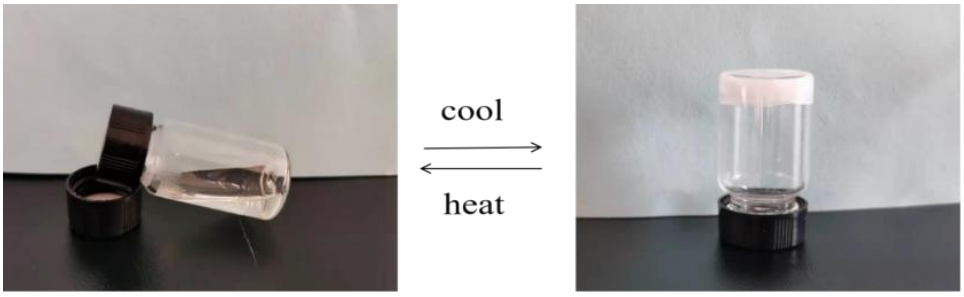

Fig. S6. The thermally reversible of the G2@gel

6. Temperature-dependent fluorescence spectra of G2@gel - Acridine red

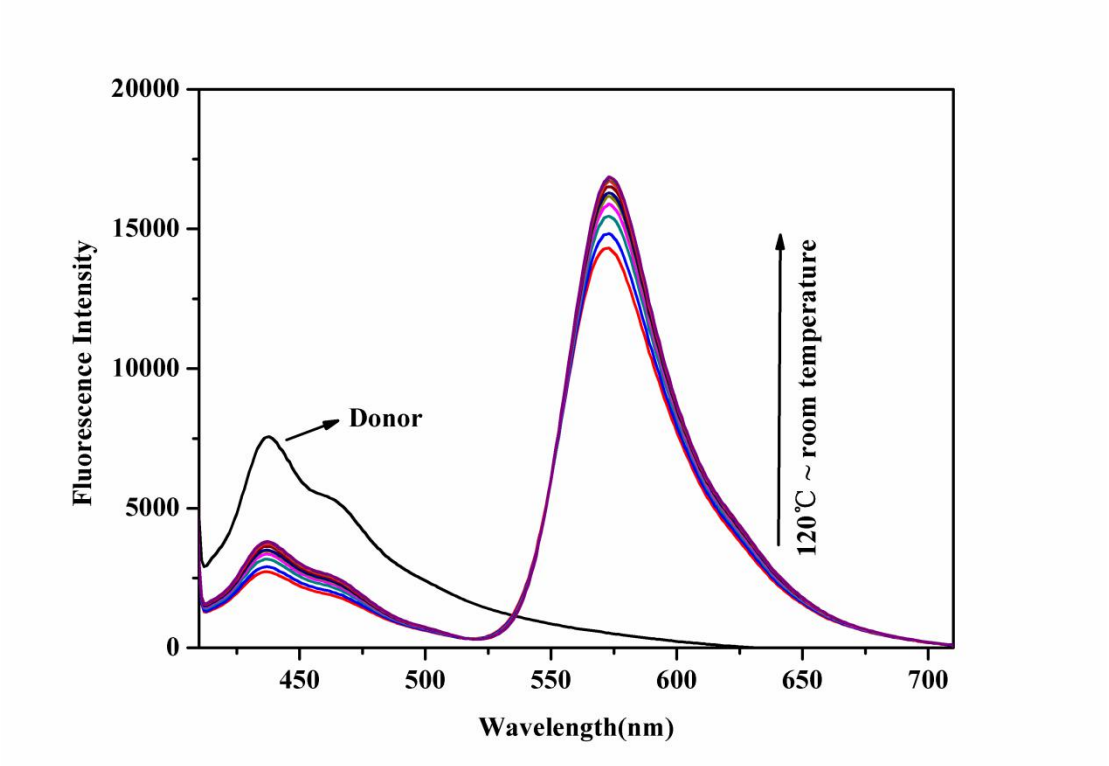

Fig. S7. Temperature-dependent fluorescence spectra (λ_{ex}=400nm) of G2@gel-Acridine red (1.0%, in glycol) during the gelation process

7. SEM and Fluorescence microscopy image

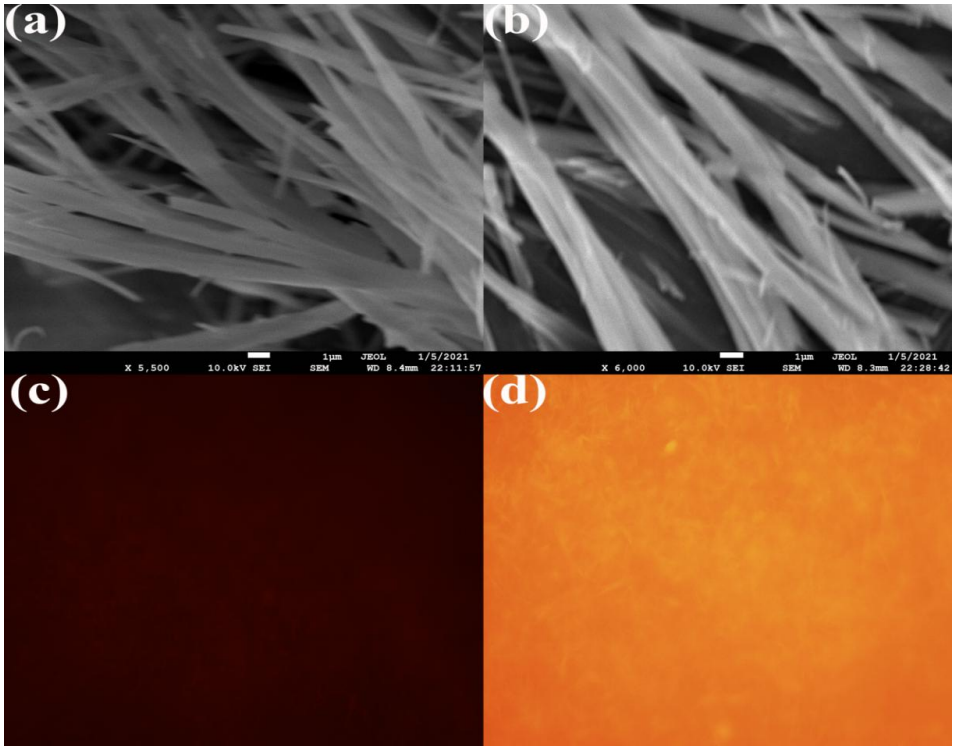

Fig. S8. (a) SEM image of G2@gel-RhB (G2@gel-RhB, 1.0%, in glycol). (b) SEM image of G2@gel-Acridine red (G2@gel-Acridine red, 1.0%, in glycol). (c) Fluorescence microscopy image of the G2@gel- RhB (G2@gel- RhB, 1.0%, in glycol). (d) Fluorescence microscopy image of the G2@gel-Acridine red.(G2@gel-Acridine red, 1.0%, in glycol)

8. Photographs of energy transfer

Fig. S9. Photographs of (a) G2@gel-RhB (1.0%, in glycol) (b) G2@gel-Acridine red (1.0%, in glycol) under the 365 nm UV irradiation with the molar ratio decreased from100:1 to 1000:1

9. **Fluorescence quantum yield**

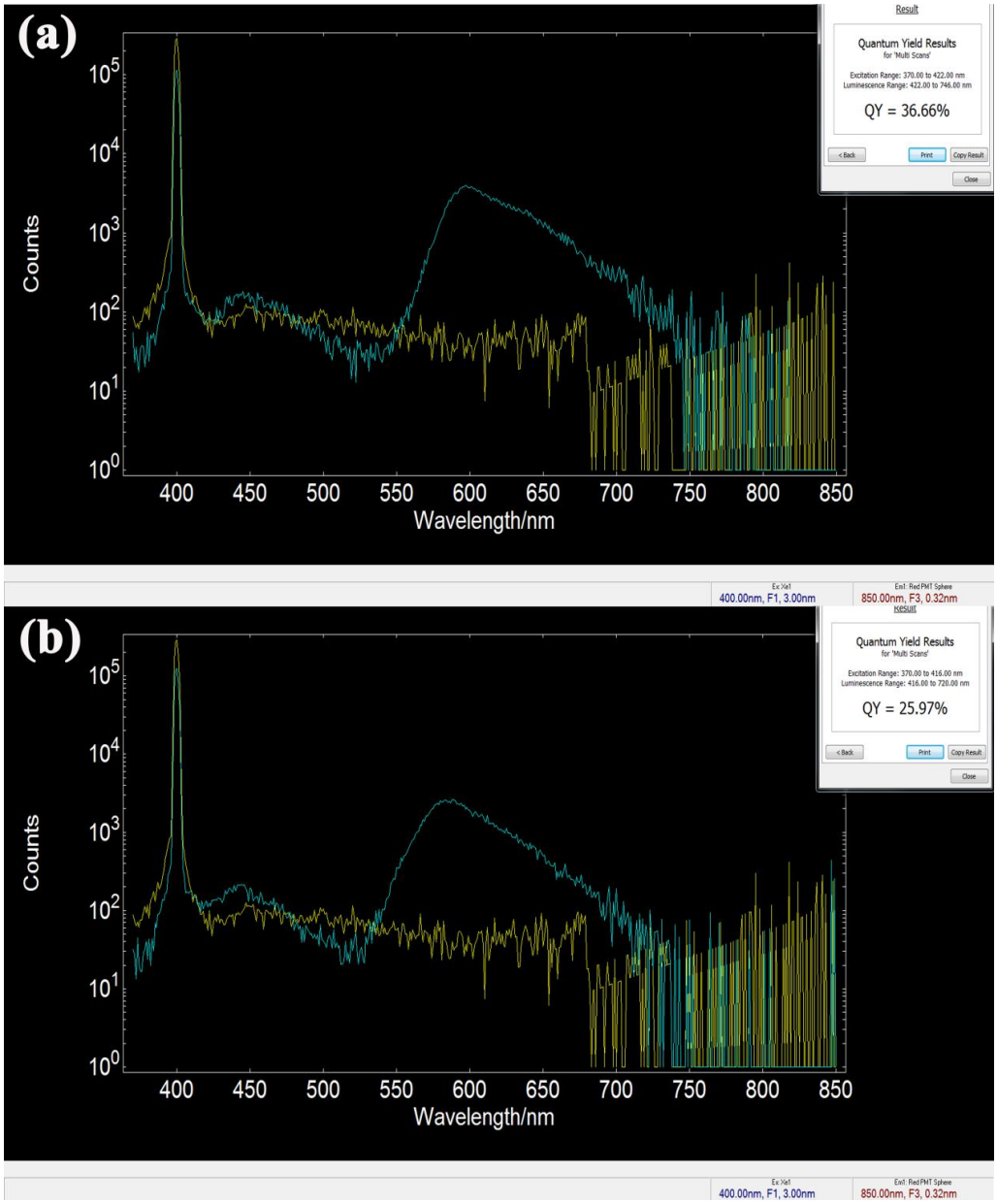

Fig. S10. (a) The fluorescence quantum yield at molar ratio of G2@gel/RhB was 100:1; (b)The fluorescence quantum yield at molar ratio of G2@gel/Acridine red was 100:1

10. Energy transfer efficiency (Φ_{ET})

The energy-transfer efficiency (Φ_{ET}) was calculated using the following equation:

$$\Phi_{ET}=1-I_{DA}/I_D^1$$

Where I_{DA} and I_D are the fluorescence intensities of the emission of G2@gel-RhB or G2@gel-Acridine red (donor and acceptor) and G2@gel (donor), respectively when excited at 400nm.

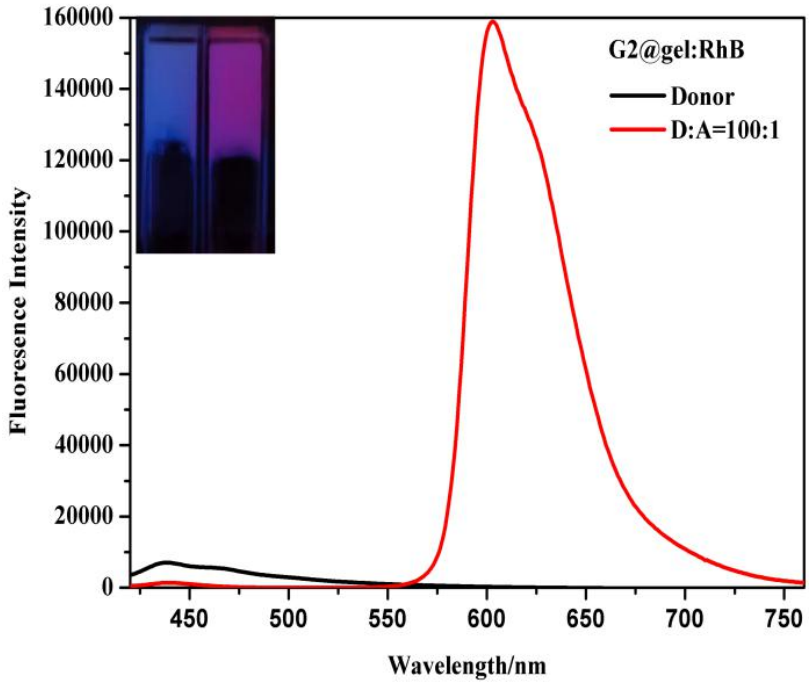

Fig. S11. Fluorescence spectra of G2@gel (1.0%, in glycol) and G2@gel-RhB (1.0%, in glycol) (λ_{ex}=400 nm). Inset: photographs of G2@gel and G2@gel-RhB under 365 nm UV light

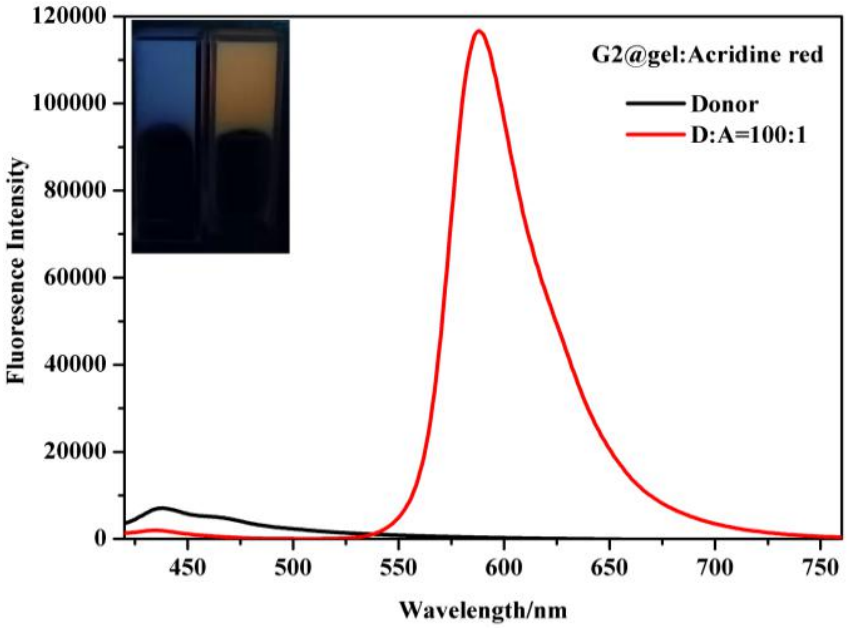

Fig. S12. Fluorescence spectra of G2@gel (1.0%, in glycol) and G2@gel-Acridine red (1.0%, in glycol) (λ_{ex}=400 nm). Inset: photographs of G2@gel and G2@gel-Acridine red under 365 nm UV light

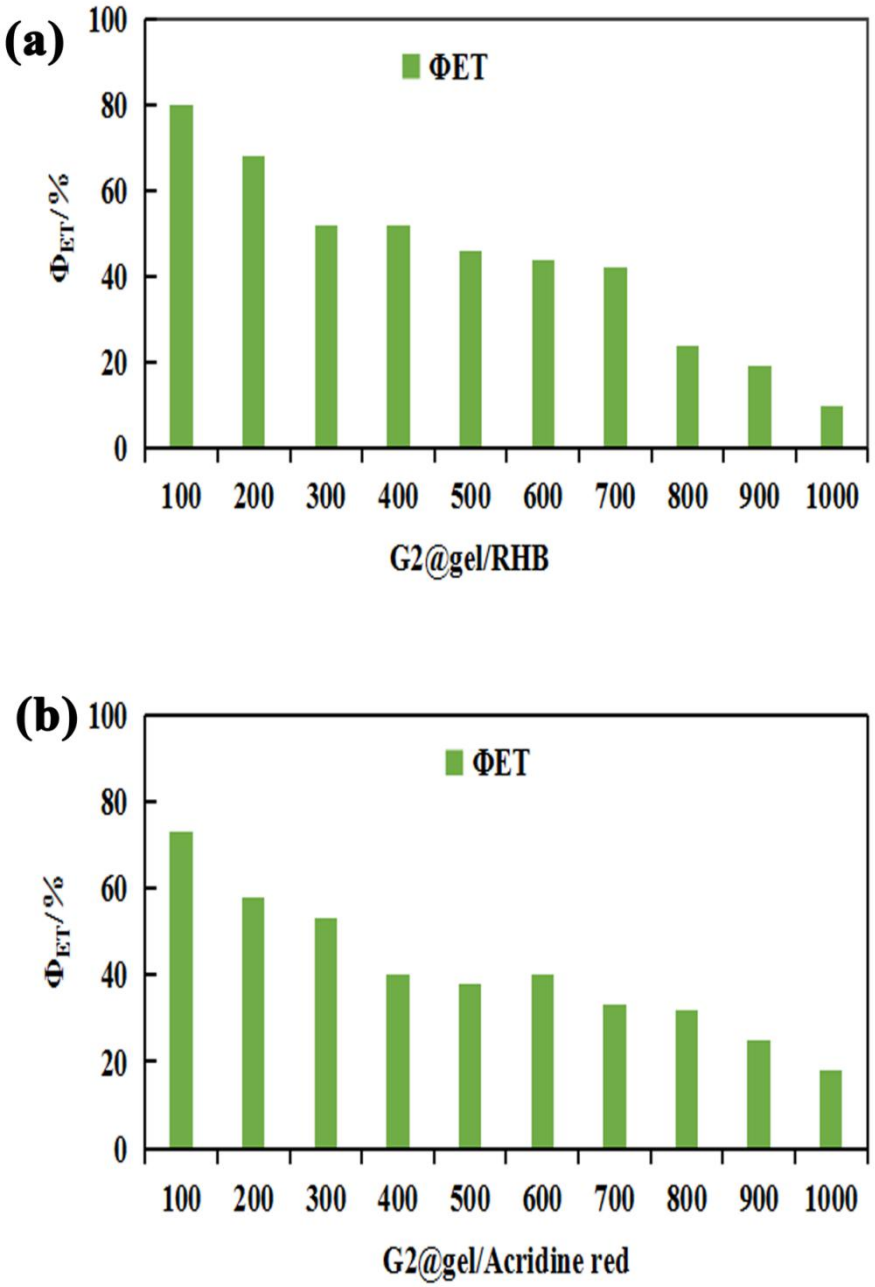

Fig. S13. (a) The energy transfer efficiency of G2@gel-RhB self-assembly at different ratios; (b) The energy transfer efficiency of G2@gel-Acridine red self-assembly at different ratios

Notes and references

1 (a) J. J. Li, H. Y. Zhang, X. Y. Dai, Z. X. Liu and Y. Liu, Chem. Commun., 2020, 56, 5949-5952; (b) G. P. Sun, W. R. Qian, J. M. Jiao, T. T. Han, Y. K. Shi, X. Y. Hu and L. Y. Wang, J. Mater. Chem. A, 2020, 8, 9590-9596